Bandwidth-control-induced insulator-metal transition in $Pr_{0.65}(Ca_{1-y}Sr_y)_{0.35}MnO_3$ and $Pr_{0.7}Ca_{0.3}MnO_3$

H. Yoshizawa and R. Kajimoto
Neutron Scattering Laboratory, Institute for Solid State Physics, University of Tokyo, Shirakata 106-1, Tokai, Ibaraki, 319-11, Japan

H. Kawano
The Institute of Physical and Chemical Research (RIKEN), Wako, Saitama 351-01, Japan

Y. Tomioka
Joint Research Center for Atom Technology (JRCAT), Tsukuba, 305, Japan

Y. Tokura
Joint Research Center for Atom Technology (JRCAT), Tsukuba, 305, Japan
and Department of Applied Physics, University of Tokyo, Tokyo 113, Japan
(Received 22 July 1996; revised manuscript received 21 October 1996)

Both internal chemical pressure by ion substitution and external hydrostatic pressure induce an insulator-to-metal (*I-M*) transition in the $Pr_{1-x}Ca_xMnO_3$ system. The behavior of spin and charge ordering through the *I-M* transition has been studied with use of neutron diffraction techniques. As a function of effective pressure, we identify three different pressure regions for the low-temperature state. [S0163-1829(97)08105-8]

Recently, pseudoperovskite manganese oxides $AMnO_3$ are under intensive studies, because some of them show, regardless of their being thin film or bulk, anomalously large negative magnetoresistance [colossal magnetoresistance CMR].[1–6] Within a framework of a double exchange (DE) mechanism,[7] an effective electron transfer $\tilde{t}$ is given by $\tilde{t}=t\cos(\theta/2)$, where t and θ denote an electron transfer probability when localized t_{2g} spins are parallel, and an angle between two neighboring t_{2g} spins, respectively. Therefore, the mobility of electrons in the DE system is expected to increase drastically by enhancing an effective electron transfer $\tilde{t}$. Indeed, the CMR phenomenon has been frequently observed near the metamagnetic transition induced by an external magnetic field.[3,4] In this case, $\tilde{t}$ is controlled through θ by aligning spins towards the field direction. On the other hand, $\tilde{t}$ is also expected to be controlled through t by changing the bond angles between transition-metal ions and oxygen ions. According to recent studies of a doped lanthanum manganite system with fixed hole concentration,[5] both hydrostatic pressure and chemical pressure yield very similar effects on t because, in essence, both change the Mn-O bond angles. It is also well known that hydrostatic pressure or alloying leads to a dramatic variation of resistivity in the case of Ni oxides.[8,9]

Because of a strong coupling of the transport property with lattice and spin freedoms in the manganite systems, it is crucial to clarify the influence of each freedom to the CMR phenomenon. Rapidly accumulating experimental data seem to suggest that a larger drastic change in resistivity is frequently observed at the *I-M* transition in the manganites with charge ordering rather than in those which never show charge ordering.[2–4,6] Therefore, it is important to consider the influence of charge ordering, although recent theoretical analyses place more emphasis on Jahn-Teller (JT) effects.[10]

Motivated by these considerations, we have performed a neutron diffraction study of the t-control-induced *I-M* transition in the $Pr_{1-x}Ca_xMnO_3$ system in order to elucidate the influence of spin and charge orderings. In the present study, the t control was achieved either by internal chemical pressure through substitution of Ca ions with Sr ions for the $Pr_{0.65}(Ca_{1-y}Sr_y)_{0.35}MnO_3$ system or by external hydrostatic pressure for $Pr_{0.7}Ca_{0.3}MnO_3$. The neutron diffraction study of the θ-control-induced *I-M* transition in $Pr_{0.7}Ca_{0.3}MnO_3$ has been reported previously.[11]

Very recently, the effects of internal pressure on $Pr_{0.65}Ca_{0.35}MnO_3$ were studied by Tomioka *et al.*,[12] while the influence of hydrostatic pressure on $Pr_{0.7}Ca_{0.3}MnO_3$ was studied by Moritomo *et al.*[13] The Sr doping effects on $Pr_{0.7}Ca_{0.3}MnO_3$ were also studied by B. Raveau *et al.*[6] For the praseodymium manganite system, the hydrostatic and chemical *pressure* effects can be discussed in parallel. We identify that there are three qualitatively different regions in behavior of resistivity as are schematically depicted at the upper panel in Fig. 1. At low pressure, both $Pr_{0.7}Ca_{0.3}MnO_3$ and $Pr_{0.65}Ca_{0.35}MnO_3$ exhibit charge ordering at T_{CO}, and remain insulating down to 0 K [region (a)].[4,14] Under the influence of intermediate *pressure*, however, they first form charge ordering, and then undergo an *I-M* transition at T_{IM} [region (b)]. With much higher *pressure*, they completely lose charge ordering and directly transform from a paramagnetic insulator to a ferromagnetic metal [region (c)]. In the present study, we shall show below that there is a complete correspondence between the behavior of resistivity and that of spin structures, and suggest a schematic phase diagram including magnetic phases shown at the bottom panel in Fig. 1. In the following, we report the results of the $Pr_{0.65}(Ca_{1-y}Sr_y)_{0.35}MnO_3$ with $y=0.3$ and 0.5 as typical examples for intermediate and high *chemical* pres-

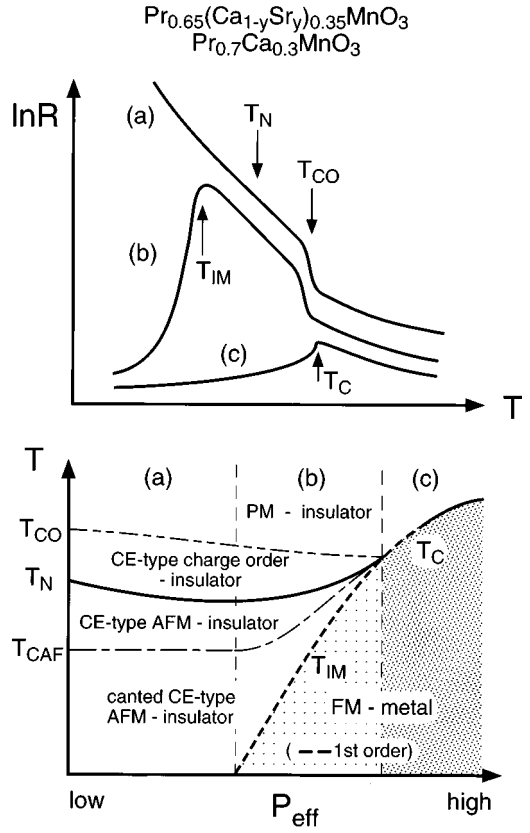

FIG. 1. Upper panel: schematic behavior of the resistivity for three regions in the $Pr_{1-x}Ca_xMnO_3$ system. Lower panel: schematic phase diagram on effective pressure vs temperature for a charge-ordered system.

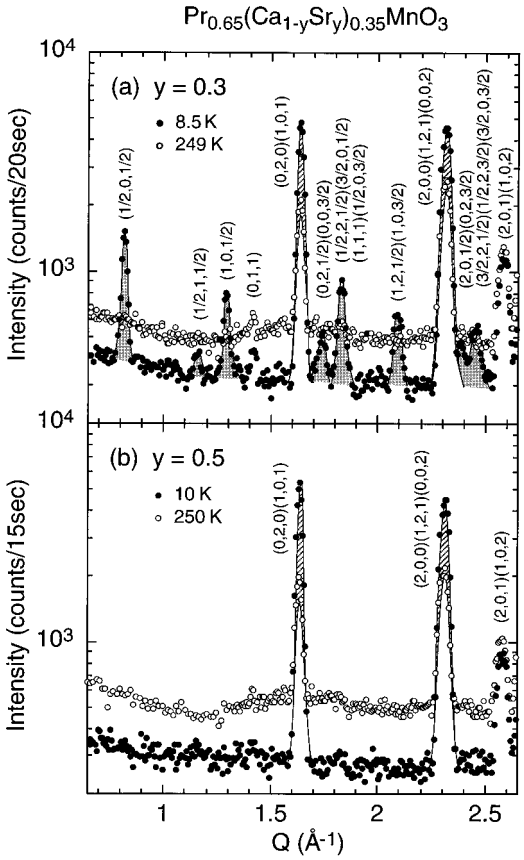

FIG. 2. Powder profiles for $Pr_{0.65}(Ca_{1-y}Sr_y)_{0.35}MnO_3$ with $y=0.3$ and 0.5. The hatched area indicates the ferromagnetic contribution to the nuclear Bragg scattering, while the shaded area in the upper panel indicates AFM superlattice reflections, respectively.

sure, while those of the $Pr_{0.7}Ca_{0.3}MnO_3$ sample with 0.2, 0.7, and 2.0 GPa as typical examples under low, intermediate, and high *hydrostatic* pressure.

Single-crystal samples were melt grown by a floating-zone method in a flow of 100% O_2 gas with a traveling speed of 3–5 mm/h. For diffraction experiments, powder samples were prepared by powdering the single crystals, and were pressed into rods. The detailed procedure of sample preparation was reported previously.[4]

Neutron diffraction measurements were performed on a triple-axis spectrometer GPTAS installed at a beam tube 4G in the JRR-3M of JAERI, Tokai. The samples $Pr_{0.7}Ca_{0.3}MnO_3$ and $Pr_{0.65}(Ca_{1-y}Sr_y)_{0.35}MnO_3$ studied in the present study belong to the space group *Pnma*. For the powder profile measurements, an incident neutron momentum $k_i=3.825$ Å^{-1} with a combination of 40′-20′-20′ collimators was utilized. For the pressure experiments, an incident neutron momentum of $k_i=2.575$ Å^{-1} and a combination of 40′-40′-40′ collimators were selected. A single-crystal sample was mounted in a pressure microcell with the [010] axis vertical to yield the $(h,0,l)$ scattering plane. A liquid of Fluorinert was filled in a microcell as a pressure-transmitting medium, and pressure was calibrated by measuring the scattering angle of the (2,0,0) Bragg reflection of a NaCl single crystal which was mounted in the microcell together with the sample crystal. To observe the behavior of the ferromagnetic (FM), antiferromagnetic (AFM), and charge order (CO) components, we performed measurements at $Q=$ (1,0,1) and (0,2,0), (0.5,0,0.5), and (2,0,1.5) or (2,0,2.5) in a similar manner with the previous study of the field effects.[11]

First, we begin with the results of the chemical-pressure-induced *I-M* transition. Neutron diffraction patterns for $Pr_{0.65}(Ca_{1-y}Sr_y)_{0.35}MnO_3$ with $y=0.3$ and 0.5 are depicted in Fig. 2. The background intensity decreases at low temperatures because intense paramagnetic scattering of Mn ions transforms into the magnetic Bragg reflections in magnetically ordered phases. According to the resistivity measurements,[12] the $y=0.3$ sample shows charge ordering below $T_{CO}\sim 205$ K and metallic conductivity below $\sim$ 80 K [region (b) in Fig. 1]. Being consistent with the DE picture, we observed clear ferromagnetic scattering on nuclear Bragg reflections at 8.5 K. In addition to the FM component, however, it exhibits clear AFM Bragg peaks of the ferromagnetically stacked CE-type AFM structure because of strong hysteretic nature of the *I-M* transition. The intensity analysis of the $y=0.3$ sample yielded the observed AFM moment of $(1.9\pm0.1)\mu_B$ which was slightly tilted from the [010] direction, but no significant difference between the Mn^{3+} and Mn^{4+} moments. The FM moment is $(2.8\pm0.1)\mu_B$, being in the ac plane. By contrast, the $y=0.5$ sample [region (c) in Fig. 1] shows no superlattice AFM reflection, but only the increase of Bragg intensity, indicating the sample is purely ferromagnetic at 10 K. The magnetic moment of the $y=0.5$ sample is $(3.5\pm0.1)\mu_B$, and lies in the ac plane, most likely along the [001] direction.

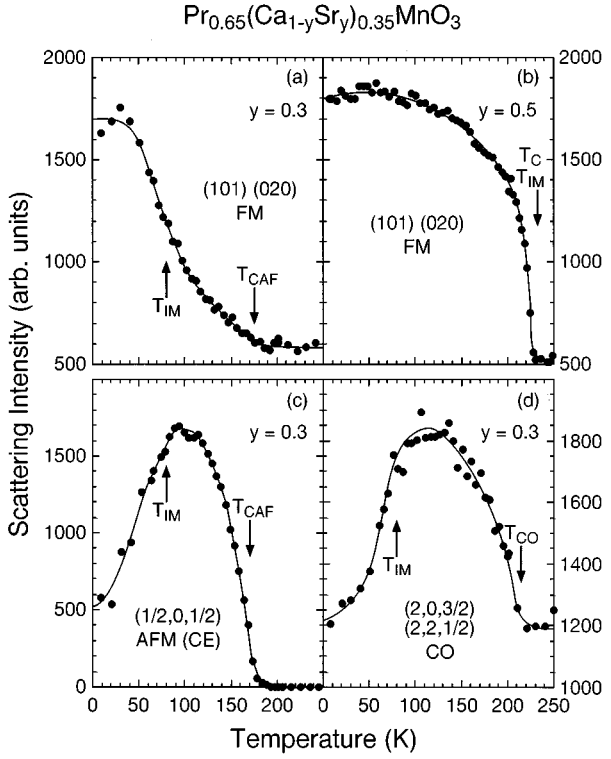

FIG. 3. Upper panels: temperature dependence of the FM components in the $y=0.3$ and 0.5 samples. Lower panels: temperature dependence of the AFM and CO components in the $y=0.3$ sample. The curves are drawn as guides to the eye.

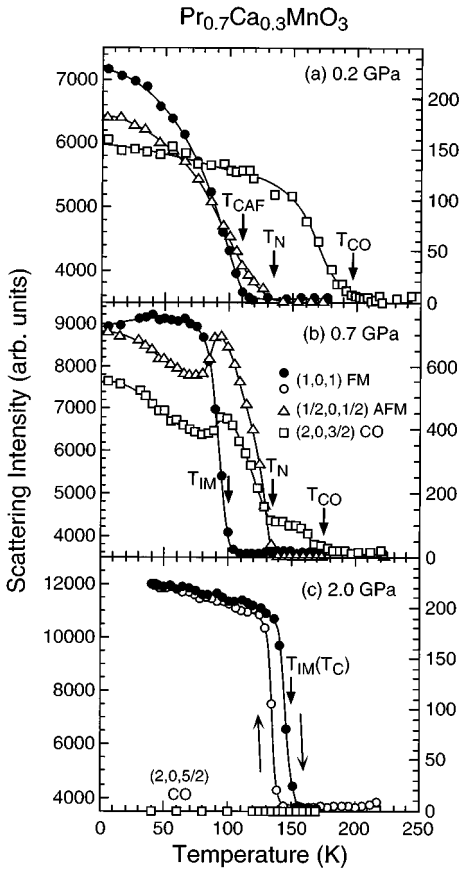

FIG. 4. Temperature dependence of the FM, AFM, and CO components for three selected pressures 0.2 (low), 0.7 (intermediate), and 2.0 (high) GPa, respectively. The curves are drawn as guides to the eye.

In the case of the $y=0.3$ sample, however, we further noticed that there existed an extremely weak additional magnetic peak which corresponds to the antiferromagnetically stacked CE-type spin structure. This coexistence of the two sets of AFM Bragg reflections in the $Pr_{1-x}Ca_xMnO_3$ system was pointed out by Jirak *et al.*[14] for the concentration with $0.3 \lesssim x \lesssim 0.5$, and it was recently reconfirmed through the measurements on the $Pr_{0.7}Ca_{0.3}MnO_3$ sample.[11]

The temperature dependence of the FM, AFM, and CO components for the $y=0.3$ and that of the FM component for the $y=0.5$ sample are shown in Fig. 3. The FM component of the $y=0.3$ sample appears at $T_{CAF} \sim 175$ K, and gradually increases with decreasing temperature. This temperature dependence is somewhat unusual compared with that of conventional FM ordering. However, such unusual behavior reflects the temperature dependence of the AFM and CO components. As shown in the lower two panels in Fig. 3, the CO in the $y=0.3$ sample sets in at $T_{CO} \sim 205$ K, and the AFM ordering appears below $T_{CAF} \sim 170$ K. With further decreasing temperature through $T_{IM} \sim 80$ K, the AFM and CO components decrease, but the FM component continues to increase. It should be noted that both AFM and CO components persist in the metallic phase below $T_{IM} \sim 80$ K, being consistent with Fig. 2. We interpret that the remanent AFM and CO components are a distinct feature due to strong hysteresis at the *I-M* transition in the *intermediate pressure* region in these manganite systems. In our recent study,[11] identical behavior was observed in the metallic phase induced by an external magnetic field. The existence of the CO component in the metallic phase of the present system was recently observed with x-ray diffraction measurements,[12] while the remanence of the AFM component in the metallic phase was reported in a slightly different concentration $Pr_{0.7}(Ca_{1-y}Sr_y)_{0.3}MnO_3$ with $y=1/6$.[6] For the $y=0.5$ sample, on the other hand, only the FM ordering sets in at $T_C \sim 215$ K, being accompanied with the *I-M* transition. The temperature dependence of the FM component is of a conventional type.

We now turn to describe the results of external pressure experiments. According to the resistivity measurements,[13] $Pr_{0.7}Ca_{0.3}MnO_3$ exhibits pressure-induced *I-M* transition for $P \gtrsim 0.5$ GPa. Three panels in Fig. 4 give the temperature dependence of the integrated intensity of the FM, AFM, and CO components at three selected pressures 0.2, 0.7, and 2.0 GPa [regions (a), (b), and (c) in Fig. 1, respectively].

The behavior of each components at 0.2 GPa was qualitatively identical with that at ambient pressure.[4,11] The CO sets in at $T_{CO} \sim 200$ K, and the AFM ordering appears below $T_N \sim 135$ K, and the FM component appears below $T_{CAF} \sim 110$ K. At 0.7 GPa in the region (b), the *I-M* transition takes place near $T_{IM} \sim 100$ K according to the resistivity measurements.[13] It is clear from Fig. 4(b) that the charge-ordered state is formed below ~ 180 K, and the AFM component appears at $T_N \sim 130$ K. The $Pr_{0.7}Ca_{0.3}MnO_3$ sample exhibits a steep rise of the FM component in the temperature range of 80–100 K, but a slight decrease of the AFM and CO

components. Note that both AFM and CO components persist in the metallic phase, being similar to the results of the $y=0.3$ sample. At 2.0 GPa [region (c)], we observed only a FM component, but neither AFM nor CO component.

Recent theory often stresses importance of JT effects. Hence, lattice anomalies and a change of Mn-O bond angles at the *I-M* transition are discussed from this viewpoint.[10] However, charge ordering can cause a larger effect on a lattice anomaly.[3,4] In the present $Pr_{0.7}Ca_{0.3}MnO_3$ system, the influence of charge ordering is manifested as a distinct lattice anomaly at the *I-M* transition under pressure. The temperature dependence of the peak position of the (1,0,1) Bragg reflection for region (b) (0.7 GPa) and that of region (c) (2.0 GPa) are depicted in Fig. 5. Although only pressure was varied between two measurements, there is a qualitative difference. Under intermediate pressure in which the *I-M* transition is accompanied with melting of CO, the peak position exhibits a sharp shift at the *I-M* transition, whereas under higher pressure in which the system shows no CO, it shows only a change of slope. This contrast clearly suggests that a huge variation of the resistivity at the *I-M* transition in the $Pr_{0.7}Ca_{0.3}MnO_3$ system is strongly affected by a release of lattice distortions due to a collapse of CO at the *I-M* transition.

In summary, we have examined the *I-M* transition induced by external or chemical pressure in the $Pr_{1-x}Ca_xMnO_3$ system. Depending on pressure, three regions are identified. At low pressure, the system is always insulating. In the intermediate-pressure region, the system undergoes an *I-M* transition with large hysteresis. At high enough pressure, the charge ordering is completely suppressed, and the system directly transforms from a paramagnetic insulator to a ferromagnetic metal. From these observations, we have suggested a schematic phase diagram shown in Fig. 1. The largest change of lattice distortions at the *I-M* transition is observed in the case where the *I-M* transition suppresses the charge ordering.

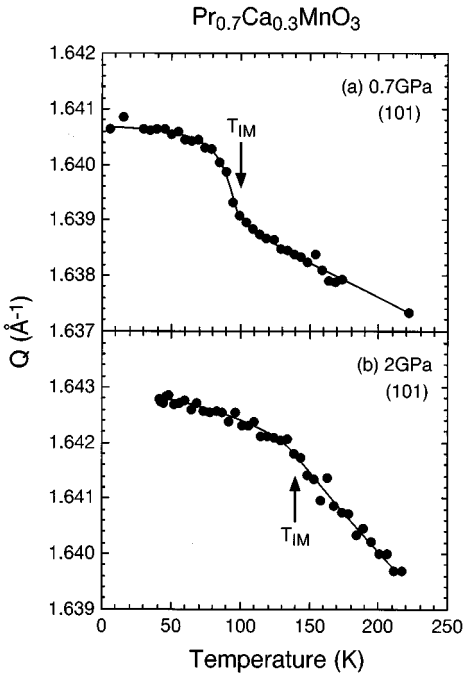

FIG. 5. Temperature dependence of the peak position of the (1,0,1) Bragg reflection at 0.7 (intermediate) and 2.0 (high) GPa, respectively. The curves are drawn as guides to the eye.

The present study was supported in part by a Grant-In-Aid for Scientific Research from the Ministry of Education, Science and Culture, Japan, and by the New Energy and Industrial Technology Development Organization (NEDO) of Japan. H.K. was supported by Special Researcher's Basic Science Program (RIKEN).

[1] R.M. Kusters *et al.*, Physica B **155**, 362 (1989); K. Chabara *et al.*, Appl. Phys. Lett. **63**, 1990 (1993); R. von Helmont *et al.*, Phys. Rev. Lett. **71**, 2331 (1993); S. Jin *et al.*, Science **264**, 413 (1994); H.L. Ju *et al.*, Appl. Phys. Lett. **65**, 2108 (1994); M. McCormack *et al.*, *ibid.* **64**, 3045 (1994).

[2] Y. Tokura *et al.*, J. Phys. Soc. Jpn. **63**, 3931 (1994); A. Urushibara *et al.*, Phys. Rev. B **51**, 14 103 (1995).

[3] Y. Tomioka *et al.*, Phys. Rev. Lett. **74**, 5108 (1995); H. Kuwahara *et al.*, Science **270**, 961 (1995); Y. Tokura *et al.*, Phys. Rev. Lett. **76**, 3184 (1996).

[4] Y. Tomioka *et al.*, J. Phys. Soc. Jpn. **64**, 3626 (1995); Y. Tomioka *et al.*, Phys. Rev. B **53**, R1689 (1996).

[5] H.Y. Hwang *et al.*, Phys. Rev. Lett. **75**, 914 (1995); H.Y. Hwang *et al.*, Phys. Rev. B **52**, 15 046 (1995).

[6] B. Raveau *et al.*, J. Solid State Chem. **117**, 424 (1995); A. Maignan *et al.*, Z. Phys. B **99**, 305 (1996); V. Caignaert *et al.*, J. Magn. Magn. Mater. **153**, L260 (1996).

[7] C. Zener, Phys. Rev. **82**, 403 (1951); P.W. Anderson and H. Hasegawa, Phys. Rev. **100**, 675 (1955); P.-G. de Gennes, *ibid.* **118**, 141 (1960).

[8] J.B. Torrance *et al.*, Phys. Rev. B **45**, 8209 (1992).

[9] X. Obradors *et al.*, Phys. Rev. B **47**, 12 353 (1993); P.C. Canfield *et al.*, *ibid.* **47**, 12 357 (1993).

[10] For example, see A. J. Millis *et al.*, Phys. Rev. Lett. **74**, 5144 (1995); H. Röder *et al.*, *ibid.* **76**, 1356 (1996); J. Zang *et al.*, *ibid.* **53**, R8840 (1996).

[11] H. Yoshizawa *et al.*, Phys. Rev. B **52**, R13 141 (1995); H. Yoshizawa *et al.*, J. Phys. Soc. Jpn. **65**, 1043 (1996).

[12] Y. Tomioka *et al.* (unpublished).

[13] Y. Moritomo *et al.* (unpublished).

[14] Z. Jirak *et al.*, J. Magn. Magn. Mater. **53**, 153 (1985).